Physics of climbing ropes - part 3: viscous and dry friction combined, rope control and experiments

English Version 1 (July 2, 2012)

Ulrich Leuthäusser

In this third paper on physics of climbing ropes the full equations of motion for a fall in a climbing rope are set up and solved when both internal viscous friction and external dry friction between the rope and one anchor point are taken into account. An essential part of the work discusses how the belayer can control the fall by adjusting the rope slip in the belay device. The theory can fully explain measurements of the maximum impact force, the force on the belayer and on the anchor point with and without rope control.

Contents

1. The rope model with viscous and dry friction

In the first paper [1] we discussed mainly the internal viscous friction of a climbing rope. In the second paper [2] the consequences of external dry friction have been analyzed. Here, both types of friction are combined. Viscous friction, dry friction and the elastic properties of the rope are necessary to calculate correctly the forces that occur during a fall with one anchor (protection) point and to explain precise measurements which are now available [3]. The paper can be read independently of the first two papers.

Before we describe our rope model in more detail, it is interesting to have a closer look at the rope on a microscopic descriptive level. A climbing rope is made of polymer fibers of the type polyamide whose molecular chains show entangled structures much like cooked spaghetti.

A single chain molecule (i.e. one spaghetti) consists of identical chemical components which can be easily untangled, i.e. straightened, by an external force. After removing the external force, the chain molecules quickly contract again which leads to high elasticity. This is due to entropy, a measure of disorder of a system. Because of entropy a polymer quickly returns to this statistically favorable, entangled state of high entropy. One therefore speaks of entropic elasticity. Because higher temperatures increase this effect, entropy is also responsible for the shrinkage of a polymer when it is heated, unlike most other materials which expand under heat (this is also the reason why climbing shoes, also made of polymers, hurt so much when the sun shines on them).

The individual chain molecules form a network mesh and (depending on the vulcanization grade) rub against each other, so that polymers also show viscous behavior in addition to their elastic behavior. This is extremely desirable, because without this internal friction there would be no energy absorption of the climbing rope.

If both elastic and viscous behavior is present, we speak of a viscoelastic material. After the removal of an external force such a material behaves similarly to an elastic material (i.e. it contracts immediately), but unlike the elastic material it returns to its original state with a time delay. This is an example of a memory effect, because although the force is already zero the viscoelastic material is still moving. Memory effects always lead to energy dissipation. In addition, the equations of motion for stress and strain in viscoelastic materials are integral equations. This rather abstract but elegant phenomenological description is equivalent to a very intuitive description by means of viscoelastic theory which is using mechanical models of springs and damping elements. In a modular way one can simulate complex behavior of viscoelastic materials with any arrangements of springs and damping elements.

Fortunately it turns out that a relatively simple SLS (Standard Linear Solid) model in form of a three-parameter model is sufficient to describe a climbing rope.

In Fig.1-1 a SLS model is applied on each side of the anchor point. It consists of two different springs and one damping element. The spring which is parallel to the damping element is responsible for the long term behavior (2-3 sec) of the rope. For the more interesting shorter times (0.1-0.3 sec) before and shortly after the maximum impact force occurs, one actually needs only two parameters for the description.

For the complete description of Fig.1-1 one needs the following parameters which can be calculated from the three length-independent material parameters E1, E2, and η:

---

[1] U. Leuthäusser, Viscoelastic theory of climbing ropes. http://www.sigmadewe.com/fileadmin/user_upload/pdf-Dateien/Physics_of_climbing_ropes.pdf

[2] U. Leuthäusser, Physics of climbing ropes: impact forces, fall factors and rope drag. http://www.sigmadewe.com/fileadmin/user_upload/pdf-Dateien/Physics_of_climbing_ropes_Part_2.pdf

[3] DAV Sicherheitsforschung: Data, measurements and fall models. Garmisch-Partenkirchen, Germany 2011

$$k_{11} = \frac{q}{L_1} E1 \qquad k_{12} = \frac{q}{L_2} E1 \qquad k_1 = \left(\frac{1}{k_{11}} + \frac{1}{k_{12}} \right)^{-1} = \frac{q}{L} E1$$

$$k_{21} = \frac{q}{L_1} E2 \qquad k_{22} = \frac{q}{L_2} E2 \qquad k_2 = \left(\frac{1}{k_{21}} + \frac{1}{k_{22}} \right)^{-1} = \frac{q}{L} E2 \qquad (1.1)$$

$$\eta_1 = \frac{q}{L_1} \eta \qquad \eta_2 = \frac{q}{L_2} \eta$$

The spring constants k_1, k_2 and the viscosity $q/L\eta$ are the parameters of the SLS model without the anchor point when the two SLS models in series are combined into one.

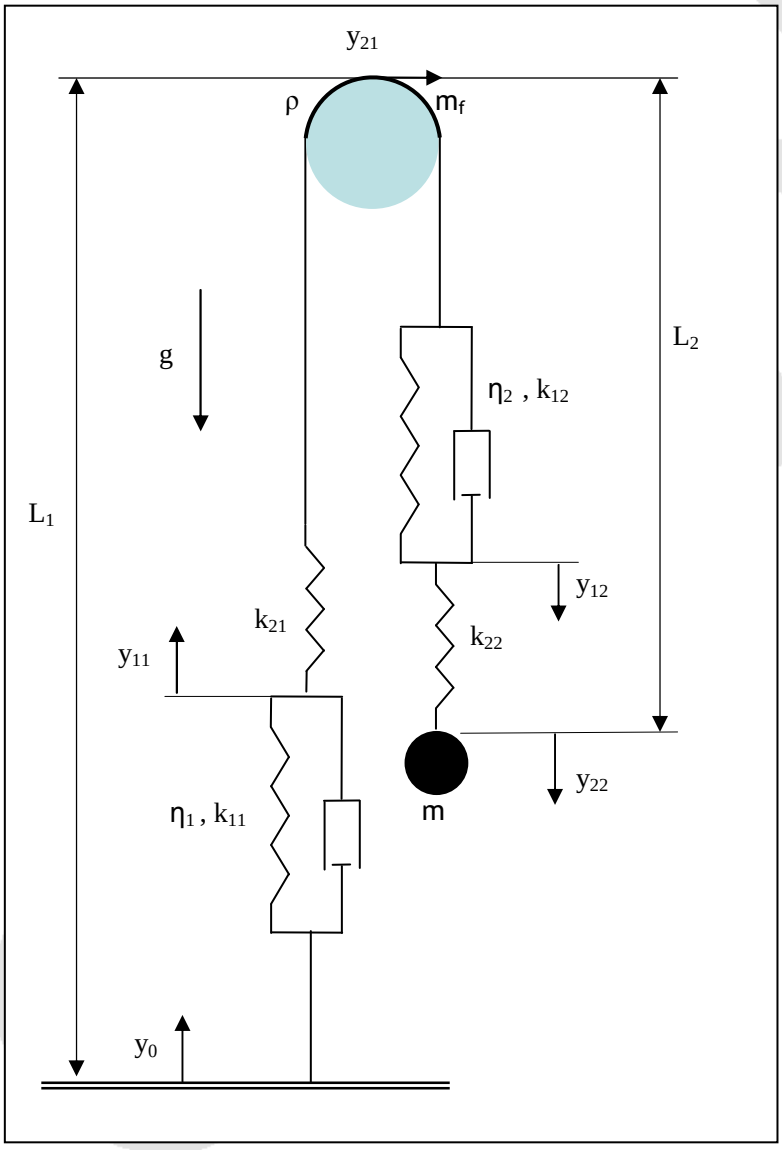

Fig.1-1: 3-parameter model: all length-dependent parameters k_{ij} and η_i (see (1.1)) are determined by 2 moduli of elasticity E1 and E2 and the viscosity η. m_f is the mass of the rope segment in the area of the anchor point. L, L_1, L_2, ρ and y_0 are explained in the text.

q is the cross section of the rope, L_1 is the length of the rope segment before the anchor point and L_2 is the length between the anchor point and the falling mass m. The total length of the rope is $L = L_1 + L_2$.

In addition there are the following variables: y_{22} describes the elongation of the rope at the position of the falling mass m, y_{21} is the displacement of the rope at the anchor point, y_{11} and y_{12} are unobservable internal variables, and y_0 is a given function of time with which the belayer can control the fall.

The orders of magnitude of the material parameters can be easily estimated:

The static modulus of elasticity $E = \frac{E_1 E_2}{E_1 + E_2}$ is determined by measuring the strain when a static mechanical stress is applied. We assume that the rope is stretched by a weight of 80 kg (the standard UIAA falling mass), and we further assume a typical static relative elongation ε_s of 7.5%. For a climbing rope with 10 mm diameter it follows

$$E = \frac{mg}{\varepsilon_s \cdot q} = 1.3 \cdot 10^8 \left[\frac{N}{m^2}\right] = 0.13\,\text{GPa}\,.$$

It is interesting to compare this result with polyamide (2-4 GPa), rubber (0.01-0.1 GPa) or hemp (35 Gpa). A climbing rope therefore has a significantly smaller modulus of elasticity than a nylon thread which is due to the complex inner helical structure of the rope.

E2 is determined by the dynamic elongation ε_d that, under standard UIAA fall conditions, is about 4 times greater than the static elongation. E2 can be estimated using (see [1])

$$E2 \approx \frac{F^{max}}{\varepsilon_d \cdot q} = \frac{2fmg}{\varepsilon_d^2 \cdot q} \approx 0.38\,\text{GPa}$$

with the fall factor f = 1.77 for UIAA standard falls and F^{max} as the maximum impact force.

Although ε_d is four times larger than ε_s, the maximum impact force is about ten times larger than the static force exerted by the standard weight (i.e., if a climber would measure his weight at the time of the maximum impact force, he would find his weight 10 times increased). So it is the other way around: a rope can be stretched statically far more than dynamically. The slower you pull, the larger is the elongation which is typical for viscoelastic materials.

The viscosity can be estimated by multiplying the elastic modulus with the typical time in which a fall occurs (a few tenths of seconds):

$$\eta \sim 3/10\,[\text{sec}] \cdot E2\,[\text{GPa}] \cong 0.1\,[\text{GPa sec}]\,.$$

This corresponds to a damping ratio of about 0.2, therefore a rope is clearly away from the aperiodic limit case where the damping ratio is equal to 1. Rubber, for example, is damped even less, and has a damping ratio between 0.01 and 0.05.

In this rope model we also take into account the external friction between the rope and the anchor point. The external friction is, in contrast to the inner friction, velocity independent and is characterized by the parameter

$$\rho = e^{\pi\mu} \qquad (1.2)$$

with the friction coefficient μ. ρ is about 0.13 according to experiments that are discussed in section 7.

2. The force system of the rope

First, we examine the rope only at the anchor point, so that the reaction force dK and the friction force dR (see Fig.2-1) must be considered. We look at a specific location on the anchor

point where there is already a contact angle α with the rope. From there an infinitesimal change in angle dα is added.

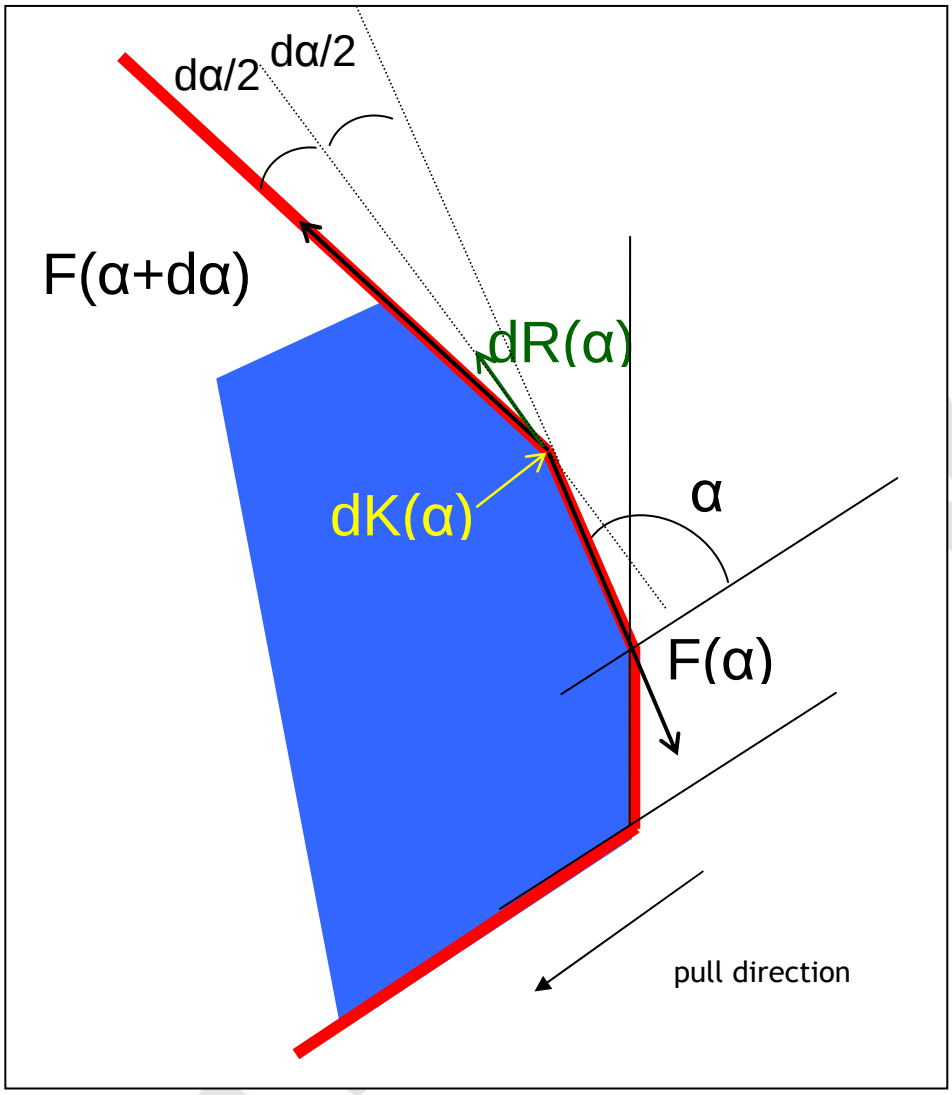

Fig. 2-1: Forces on a section of the rope at an anchor point which is not necessarily circular. α is the contact angle at a specific location of the anchor point (e.g. as a function of arc length) and contains all angular changes of the rope up to there.

Parallel to dR(α) we get for dα: $-F(\alpha+d\alpha)-dR(\alpha)+F(\alpha)=0$ and

perpendicular to dR(α) we have $-F(\alpha+d\alpha)\frac{d\alpha}{2}-F(\alpha)\frac{d\alpha}{2}+dK(\alpha)=0$.

With the friction force dR = μ·dK it follows $dK(\alpha)=F(\alpha)d\alpha=1/\mu\, dR(\alpha)$ and with the first of the two equations above follows $F(\alpha)+dF(\alpha)=F(\alpha)-\mu F(\alpha)d\alpha$ or $\frac{dF}{F}=-\mu d\alpha$. The solution of this equation is

$$F(\alpha)=F_0\exp(-\mu\alpha) \qquad (2.1)$$

known as the Euler-Eytelwein formula. The summation of all infinitesimal friction forces dR(α) yields:

$$R(\alpha) = \int_0^{\alpha} dR = F_0 (1 - \exp(-\mu\alpha)) \qquad (2.2)$$

Using the force balance equation $-F_0 + F(\alpha) + \int_0^{\alpha} dR = -F_0 + F(\alpha) + R(\alpha) = 0$ it can be seen that the difference of the pulling force F_0 and the holding force $F(\alpha)$ is equal to the sum of all frictional forces on the contact surface of anchor point and rope.

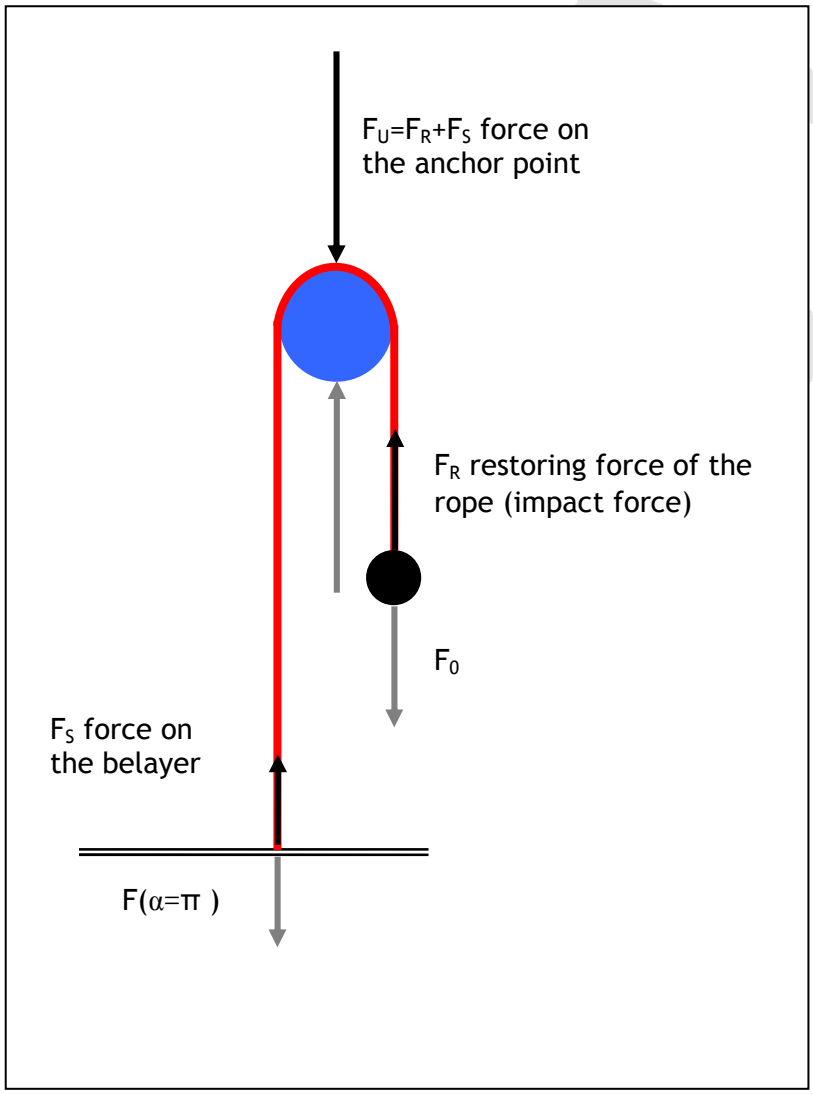

Fig.2-2: Forces of the system "anchor point + rope": on the belay (F_S), on the anchor point (F_U), and on the rope (F_R). The frictional force is an internal force of the system "anchor point + rope" and does not appear.

The force $-F_0$, called F_R (see Fig.2-2), is the restoring force of the rope acting at the end of the rope with the falling mass. Although it is not an impact in the physical sense, F_R is commonly called impact force. The force on the belay is $-F(\alpha = \pi)$ and is called F_S herein. The force on the anchor point is the sum of both forces $F_U = F_S + F_R$, which immediately follows from the equilibrium of forces of the simple geometric situation $\alpha = \pi$ in Fig.2-2. For $\alpha = \pi$ we also obtain for the frictional force

$$R = F_S - F_R \tag{2.3}$$

By means of the above formulas one gets for the motion in the direction of the fall

$$\begin{aligned} F_S &= \frac{1}{\rho} F_R \\ R &= F_S - F_R = F_S - F_S\rho = F_S(1-\rho) = F_R \frac{1-\rho}{\rho} \\ F_U &= F_R\left(1+\frac{1}{\rho}\right) \end{aligned} \tag{2.4}$$

with $\rho = e^{\pi\mu}$. Equations (2.4) are valid for the important maxima of F_S and F_R. For the motion in the opposite direction, however, there is

$$R = F_S - F_R = F_R\rho - F_R = F_R(\rho - 1) \tag{2.5}$$

In the direction of the fall and for large friction ($\rho >> 1$) it follows $R = -F_R$, i.e. $F_S = 0$. Thus, the force on the belay disappears, and in turn the force on the anchor point is two times F_R:

$$F_U = \begin{cases} 2F_R & \rho = 1, \text{ zero friction} \\ F_R & \rho >> 1, \text{ large friction} \end{cases}$$

3. The equations of motion

The easiest way to obtain the equations of motion for the situation in Fig. 1-1 is using the formalism of Lagrange [4]. The first part of the Lagrange equation L

$$\begin{aligned} L = &\frac{1}{2} m \cdot \dot{y}_{22}^{\,2} + \frac{1}{2} m_f \cdot \dot{y}_{21}^{\,2} - \\ &\left[\frac{1}{2} k_{22}(y_{22} - y_{12})^2 + \frac{1}{2} k_{12}(y_{12} - y_{21})^2 + \frac{1}{2} k_{21}(y_{21} - y_{11})^2 + \frac{1}{2} k_{11}(y_{11} - y_0)^2 - mgy_{22}\right] \end{aligned} \tag{3.1}$$

consists of the kinetic energy of the falling mass m and the mass of the piece of rope m_f in the vicinity of the anchor point. The second part is the potential energy (square bracket of 3.1) in the form of various elastic strain energies and the potential energy of the falling mass in the gravitational field. The total friction is taken into account by the dissipation function D:

[4] e.g.: D. A. Wells, Lagrangian Dynamics. Schaum's Outline Series, McGraw-Hill.

$$D = \frac{1}{2}\eta_1(\dot{y}_{11} - \dot{y}_0)^2 + \frac{1}{2}\eta_2(\dot{y}_{12} - \dot{y}_{21})^2 + |\dot{y}_{21}|(\rho - 1)\min\left(|k_{21}(y_{21} - y_{11})|, |k_{22}(y_{22} - y_{12})|\right)$$

By means of the Lagrange equations $\frac{d}{dt}\frac{\partial L}{\partial \dot{y}_i} = \frac{\partial L}{\partial y_i} - \frac{\partial D}{\partial \dot{y}_i}$, applied to all y_{ij}, one obtains the following equations of motion

$$\begin{aligned}
&m\ddot{y}_{22} + k_{22}(y_{22} - y_{12}) = mg \\
&\eta_2(\dot{y}_{12} - \dot{y}_{21}) + k_{12}(y_{12} - y_{21}) + k_{22}(y_{12} - y_{22}) = 0 \\
&\eta_1(\dot{y}_{11} - \dot{y}_0) + k_{11}(y_{11} - y_0) + k_{21}(y_{11} - y_{21}) = 0 \\
&m_f\ddot{y}_{21} + k_{21}(y_{21} - y_{11}) + k_{22}(y_{12} - y_{22}) - R = 0
\end{aligned} \qquad (3.2)$$

with the frictional force

$$R = -\frac{\dot{y}_{21}}{|\dot{y}_{21}|}(\rho - 1)\min\left(|k_{21}(y_{21} - y_{11})|, |k_{22}(y_{22} - y_{12})|\right) = -\frac{\dot{y}_{21}}{|\dot{y}_{21}|}(\rho - 1)\min\left(|F_S|, |F_R|\right) \qquad (3.3)$$

which contains the forces $F_R = -k_{22}(y_{22} - y_{12})$ and $F_S = k_{21}(y_{21} - y_{11})$.

For the case $\dot{y}_{21} > 0$ R corresponds exactly to the second equation of (2.4) and for $\dot{y}_{21} < 0$ to the equation (2.5).

If one neglects the viscous forces, the above system of equations (3.2) can be well understood without the Lagrange formalism by setting up the balance of forces at the positions y_{11}, y_{21}, y_{12} and y_{22} (see Fig. 1-1).

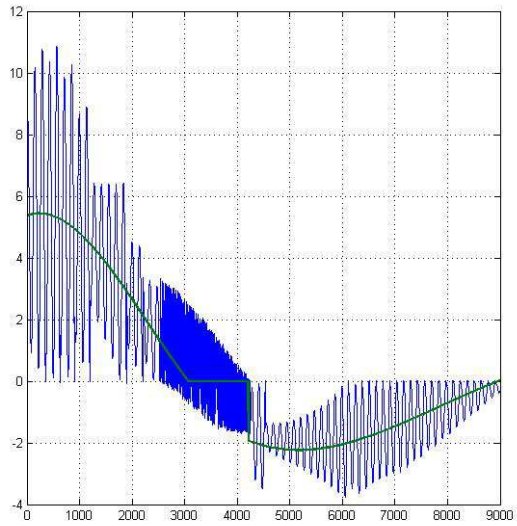

Fig.3-1: v_{21} as a function of time [10^{-4} sec] for m_f =0 (green) and m_f = 0.06 kg (blue).

In equations (3.2), fast oscillations in the velocities $\dot{y}_{21}$ and $\dot{y}_{12}$ appear (see Fig.3-1) because of the small mass m_f. This can easily lead to errors when the step size of the numerical integration routine is chosen too large.

In addition, one cannot exactly determine how long the piece of rope at the anchor point, and thus its mass m_f, has to be. It is certainly less than 1 meter, which means a very small, negligible mass $m_f < 0.06$ kg.

In section 4, therefore, the equations (3.2) are solved for $m_f = 0$. We made sure that the results are the same for the crucial parameters y_{22}, a_{22} and v_{22} regardless of whether they have been obtained for small m_f or for m_f exactly zero.

3.1. Special cases

Here the reference to the already discussed equations of the first two papers will be made.

3.1.1. $m_f = 0$ and internal friction equal to zero

The internal friction can become zero in two different ways, either viscosity $\eta = 0$ or viscosity $\eta \to \infty$.

For $m_f = 0$ and $\eta = 0$, as well as for times up to the maximum impact force the frictional force is $R = -k_{21}(\rho - 1)(y_{21} - y_{11})$ and one obtains

$$m\ddot{y}_{22} + \frac{k_{22}k_{12}}{k_{22} + k_{12}}(y_{22} - y_{21}) = mg$$

$$\frac{k_{21}k_{11}}{k_{21} + k_{11}}(y_{21} - y_0) = \frac{1}{\rho}\frac{k_{22}k_{12}}{k_{22} + k_{12}}(y_{22} - y_{21}) \qquad (3.4)$$

These are the equations (4) of "Physics of Climbing Ropes" [2] considering that the spring constants in series, k_{11} and k_{21} resp. k_{22} and k_{12}, must be replaced by the spring constants

$K_1 = \frac{k_{21}k_{11}}{k_{21} + k_{11}}$ and $K_2 = \frac{k_{22}k_{12}}{k_{22} + k_{12}}$. Eliminating also y_{21} yields ($m_f = 0$ and $\eta = 0$)

$$m\ddot{y}_{22} + \frac{\rho K_1 K_2}{\rho K_1 + K_2}(y_{22} - y_0) = mg \qquad (3.5a)$$

For $\eta \to \infty$ we obtain the same result as above but with different spring constants, because by a large η the spring constant k_{11} and k_{12} become ineffective, so that

$$m\ddot{y}_{22} + \frac{\rho k_{22}k_{21}}{\rho k_{21} + k_{22}}(y_{22} - y_0) = mg\,. \qquad (3.5b)$$

3.1.2. External friction R = 0

For R = 0 and by elimination of y_{21} and y_{11} the system of equations (1) of the work "Viscoelastic theory of climbing ropes" [1] is obtained

$$m\ddot{y}_{22} + \frac{k_{22}k_{21}}{k_{22}+k_{21}}(y_{22}-y_{12}) = mg$$

$$\frac{\eta_2\eta_1}{\eta_2+\eta_1}(\dot{y}_{12}-\dot{y}_0) + \frac{k_{12}k_{11}}{k_{12}+k_{11}}(y_{12}-y_0) + \frac{k_{22}k_{21}}{k_{22}+k_{21}}(y_{12}-y_{22}) = 0 \qquad (3.6)$$

It should be noted, however, that this does not apply for arbitrary η_1 and η_2, but only if the relation $\frac{\eta_1}{\eta_2} = \frac{L_2}{L_1}$ is valid.

3.1.3. Large external friction

For $\rho >> 1$ y_{21} can no longer move, i.e. $y_{21} = 0$ and the following equations apply

$$\begin{aligned} &m\ddot{y}_{22} + k_{22}(y_{22}-y_{12}) = mg \\ &\eta_2(\dot{y}_{12}) + k_{12}y_{12} + k_{22}(y_{12}-y_{22}) = 0 \end{aligned} \qquad (3.7)$$

y_0 no longer appears, thus the belayer has no possibility of control.

4. System of equations for $m_f = 0$ and its solution

Setting $m_f = 0$ in (3.2), one obtains the following system of equations

$$m\ddot{y}_{22} + k_{22}(y_{22}-y_{12}) = mg$$

$$\dot{y}_{21} = |\dot{y}_{21}|\frac{k_{22}(y_{22}-y_{12}) - k_{21}(y_{21}-y_{11})}{(\rho-1)\min(|k_{21}(y_{21}-y_{11})|, |k_{22}(y_{22}-y_{12})|)} \qquad (4.1)$$

$$\eta_2(\dot{y}_{12}-\dot{y}_{21}) + k_{12}(y_{12}-y_{21}) + k_{22}(y_{12}-y_{22}) = 0$$

$$\eta_1(\dot{y}_{11}-\dot{y}_0) + k_{11}(y_{11}-y_0) + k_{21}(y_{11}-y_{21}) = 0$$

The restoring force of the rope is given by $F_R = -k_{22}(y_{22}-y_{12}) = -(mg - m\ddot{y}_{22})$.

The force on the belay is $F_S = k_{21}(y_{21}-y_{11})$.

The frictional force R is given by $R = k_{21}(y_{21}-y_{11}) + k_{22}(y_{12}-y_{22}) = F_S - F_R$.

The force on the anchor point is $F_U = k_{21}(y_{21}-y_{11}) + k_{22}(y_{22}-y_{12}) = F_S + F_R$.

The system of equations (4.1) can be simplified as follows. If the falling mass has the initial velocity $\dot{y}_{22}(0) = v_0$ (at the start of elongation), then one gets for times 0 <t <t_1 (the time of the maximum of y_{21})

$$k_{22}(y_{22} - y_{12}) > k_{21}(y_{21} - y_{11}) > 0 \quad \text{and} \quad \dot{y}_{21} > 0$$

Therefore, we obtain for the frictional force $R = -(\rho - 1) \cdot k_{21}(y_{21} - y_{11})$ and hence

$$y_{21} = \frac{k_{22}}{k_{21}} \frac{1}{\rho}(y_{22} - y_{12}) + y_{11} \tag{4.2a}$$

After the time t_2, $\dot{y}_{21}$ becomes negative and the relation $k_{21}(y_{21} - y_{11}) > k_{22}(y_{22} - y_{12}) > 0$ (see Fig.4-1) applies, so the frictional force is $R = (\rho - 1) \cdot k_{22}(y_{22} - y_{12})$. y_{21} is then given by

$$y_{21} = \frac{k_{22}}{k_{21}} \rho(y_{22} - y_{12}) + y_{11} \tag{4.2b}$$

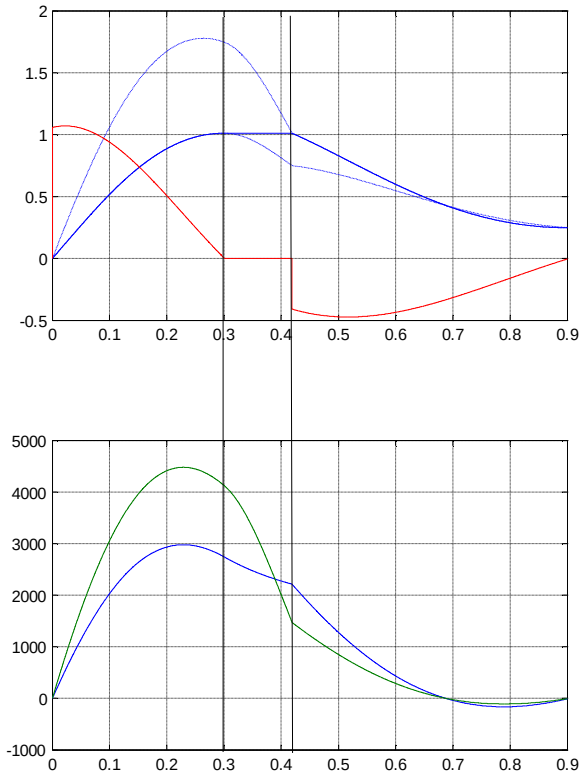

Fig.4-1a: Time curve of y_{21} (blue) with the 2 dashed curves on which y_{21} can be located and between which a horizontal transition takes place. The red curve is v_{21}. The vertical lines indicate the times t_1 and t_2.
Fig.4-1b: The force $k_{22}(y_{22} - y_{12})$ acting on the right side of the anchor point (green) and the force $k_{21}(y_{21} - y_{11})$ acting on the left side of the anchor point (blue).

Between t_1 and t_2, y_{21} of (4.2a) remains unchanged at its maximum, with t_2 determined by the intersection of y_{21} from (4.2a) with y_{21} from (4.2b). If $\dot{y}_{21} \neq 0$, the only possibility would be to either continue moving on (4.2a) or to make a vertical transition from (4.2a) to (4.2b), both of which are physically unreasonable.

Therefore one obtains

$$y_{21} = \begin{cases} \frac{k_{22}}{k_{21}} \frac{1}{\rho}(y_{22} - y_{12}) + y_{11} & 0 < t < t_1 \\ \frac{k_{22}}{k_{21}} \frac{1}{\rho}(y_{22}(t_1) - y_{12}(t_1)) + y_{11}(t_1) & t_1 < t < t_2 \\ \frac{k_{22}}{k_{21}} \rho(y_{22} - y_{12}) + y_{11} & t > t_2 \end{cases} \tag{4.2c}$$

and for the velocity of y_{21}

$$v_{21} = \begin{cases} \frac{k_{22}}{k_{21}} \frac{1}{\rho}(v_{22} - v_{12}) + v_{11} & 0 < t < t_1 \\ 0 & t_1 < t < t_2 \\ \frac{k_{22}}{k_{21}} \rho(v_{22} - v_{12}) + v_{11} & t > t_2 \end{cases} \tag{4.3}$$

$v_{21} = 0$ does not imply R = 0, but instead of dynamic friction there is now static friction.

This leads to 3 cases for

$v_{11} = \dot{y}_{11} = \frac{1}{\eta_1}(-(k_{11} + k_{21})y_{11} + k_{21}y_{21} + k_{11}y_0) + v_0$ and for

$v_{12} = \frac{1}{\eta_2}(k_{12}(y_{21} - y_{12}) + k_{22}(y_{22} - y_{12})) + v_{21}$

In the last expression, v_{12} still appears in $v_{21} = f(v_{12})$ on the right side, therefore one has yet to solve the equation for v_{12} which can easily be done.

With v_{12}, v_{11} and y_{21} the equations of motion

$$\begin{aligned} \dot{y}_{12} &= v_{12} \\ m\ddot{y}_{22} + k_{22}(y_{22} - y_{12}) &= mg \\ \eta_1(\dot{y}_{11} - \dot{y}_0) + k_{11}(y_{11} - y_0) + k_{21}(y_{11} - y_{21}) &= 0 \end{aligned} \tag{4.4}$$

can now be solved with the initial conditions

$y_{ij}(0) = 0$ and $\dot{y}_{ij}(0) = 0$ for all i, j, except $\dot{y}_{22}(0) = v_0$

v_0 is the velocity of the falling mass when the rope begins to stretch. In Section 7, the solution of (4.4) is compared with experimental data.

In the figure below the maximum impact force, the maximum force on the belay and their sum were calculated with (4.4) and are plotted as a function of the friction coefficient μ.

It is remarkable that, regardless of the internal friction η, the maximum force on the anchor point depends only slightly on the external friction, while the impact force increases sharply with μ and thus the force on the belay is decreasing.

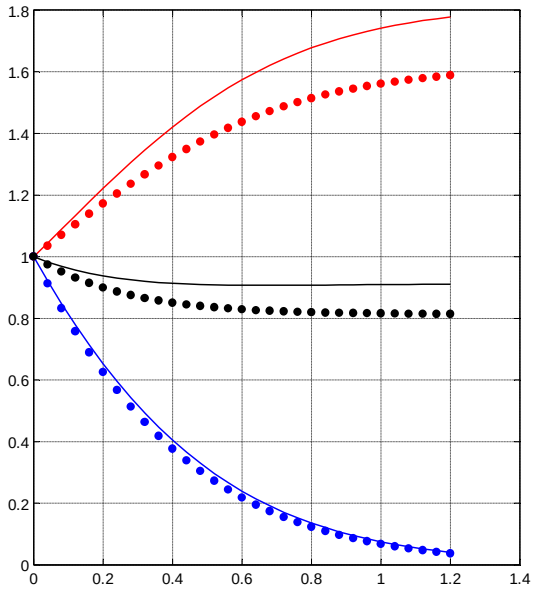

Fig.4-2: The 3 maximum forces F_R^{max} (red), F_S^{max} (blue) and F_U^{max} (black) as a function of the friction coefficient μ and related to their value at μ=0 The dotted curves are the analytically available values for $\eta \to \infty$.

The explicit expressions of the maxima of these forces for $\eta \to \infty$ (dotted lines in Fig.4-2), using the effective spring constant $k_{eff} = \frac{\rho k_{21} k_{22}}{\rho k_{21} + k_{22}}$, are given by:

$$F_R^{max} = mg + m\sqrt{v_0^2 \frac{k_{eff}}{m} + g^2}\,, \qquad F_S^{max} = \frac{1}{\rho} F_R^{max}\,, \qquad F_U^{max} = F_R^{max} + F_S^{max}$$

The analysis up to the maximum impact force can be continued still further. As already shown, up to the maximum impact force equation (4.2) applies

$y_{21} = \frac{k_{22}}{k_{21}} \frac{1}{\rho} (y_{22} - y_{12}) + y_{11}$. Inserted in the last equation of (4.4) we obtain

$\rho\eta_1 \dot{y}_{11} + \rho k_{11} y_{11} - k_{22}(y_{22} - y_{12}) = 0$. Using the transformation $k'_{11} = \rho k_{11}$, $k'_{21} = \rho k_{21}$, $\eta'_1 = \rho\eta_1$ and leaving k_{22}, k_{12} and η_2 unchanged, the equations are brought in the form with ρ = 1 (no external friction present). Thus, for short times the external friction increases the rope parameters k_{11}, k_{21} and η_{11} in front of the anchor point and one can consider the rope without taking this point explicitly into account.

With this transformation the results of the work "Viscoelastic theory of climbing ropes" [1] can thus be used. One gets for the short-term development of the acceleration $\ddot{y}_{22}$

$$\ddot{y}(t) = g - \frac{v0}{m}\frac{k_{22}\rho k_{21}}{k_{22}+\rho k_{21}}t + \frac{v0}{m}\frac{\left(\frac{k_{22}\rho k_{21}}{k_{22}+\rho k_{21}}\right)^2}{\left(\frac{\rho\eta_1\eta_2}{\rho\eta_1+\eta_2}\right)}\frac{t^2}{2} + O(t^3)$$

5. Energy dissipation

The energies per unit time which are dissipated by internal and external friction are given by

$$\dot{E}_A^V = \eta_1 \dot{y}_{11}{}^2 + \eta_2(\dot{y}_{12} - \dot{y}_{21})^2$$
$$\dot{E}_A^D = |\dot{y}_{21}|(\rho - 1)\min\left(|k_{21}(y_{21} - y_{11})|, |k_{22}(y_{22} - y_{12})|\right)$$

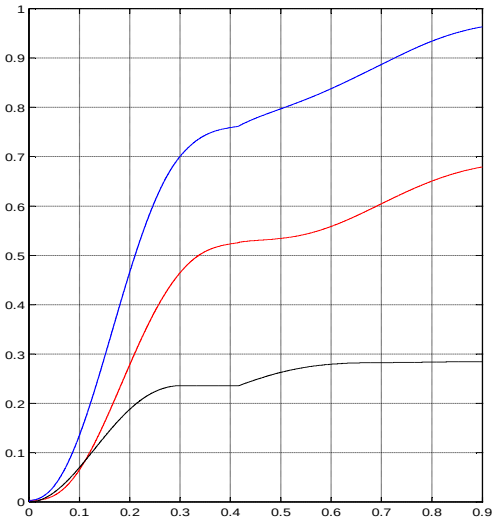

Fig.5-1: The dissipated energy components of the external friction $E_A^D(t)$ (black), the internal, viscous friction $E_A^V(t)$ (red) and their sum $E_A(t) = E_A^V(t) + E_A^D(t)$ (blue) up to time t. They are related to the total energy such that E_A goes towards one for t >> 1 sec.

For the parameters used here (see Section 7, equation (7.1)) the proportion of the external friction energy is about 1/3.

6. Rope control by the belayer

The aim of the rope control by the belayer is to minimize, for a given rope slip, the maximum force on the rope resp. on the climber.

For this purpose we first discuss a simple, analytically calculable model without internal friction. Then the general equations of motion (4.1) or (4.4) are used to numerically determine the effect of rope control on the impact force.

6.1. A simple model with rope slip y_0 and no internal friction

The used terminology from control resp. optimization theory [5] is not accidental, because the mathematical approach is just the same.

We start with equation (3.5): $m\ddot{y}_{22} + \frac{\rho K_1 K_2}{\rho K_1 + K_2}(y_{22} - y_0) = mg$. Omitting the index of y and using the abbreviation $\omega = \sqrt{\frac{1}{m}\frac{\rho K_1 K_2}{\rho K_1 + K_2}}$, we obtain

$$\ddot{y} + \omega^2 (y - y_0) = g \tag{6.1}$$

The initial conditions are $y(0) = 0, \dot{y}(0) = v_0$.

We take a control function as simple as possible so that an analytic solution of (6.1) is possible: the rope slip $y_0(t)$ begins at a time t_0, runs at constant speed u through the belay device and stops at time t_e (see Fig.6.1).

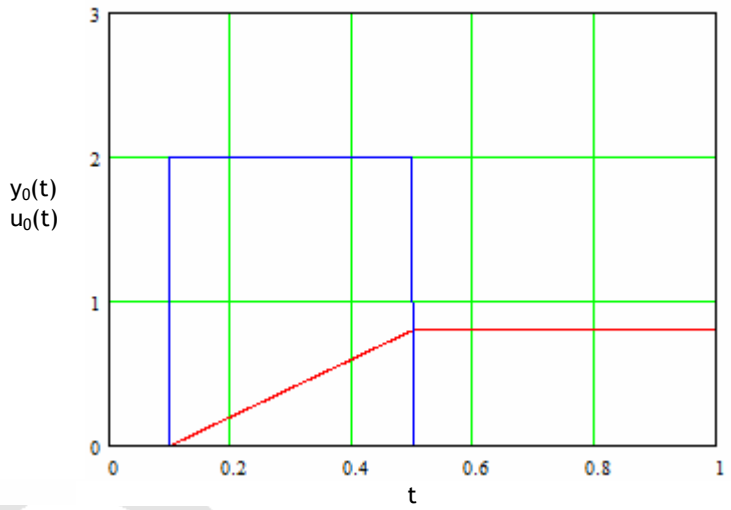

Fig.6-1: $y_0(t)$ (red) and $u_0(t)$ (blue)

Mathematically this can be expressed as:

$$\begin{aligned} y_0(t) &= \Phi(t - t_0)\Phi(t_e - t)\cdot u\cdot(t - t_0) + u\cdot(t_e - t_0)\Phi(t - t_e) \\ u_0(t) &= \Phi(t - t_0)\Phi(t_e - t)\cdot u \end{aligned} \tag{6.2}$$

The step function $\Phi(t)$ is given by: $\Phi(t) = \begin{cases} 0 & t < 0 \\ 1 & t \geq 0 \end{cases}$

[5] e.g.: M. Papageorgiou, Optimierung. Oldenbourg Verlag 1991 or
A. Bryson, Dynamic Optimazation. Addison-Wesley 1999

(6.1) can be solved by means of a Laplace transformation which leads to

$$y(t,u) = y^0(t) + u \cdot \Phi(t-t_0)\left[t - t_0 - \frac{\sin(\omega(t-t_0))}{\omega}\right] - u \cdot \Phi(t-t_e)\left[t - t_e - \frac{\sin(\omega(t-t_e))}{\omega}\right]$$
$$y^0(t) = \frac{g}{\omega^2}(1-\cos(\omega t)) + \frac{v_0}{\omega}\sin(\omega t) \qquad (6.3)$$

where $y_0(t)$ is the solution without rope control (u=0). The acceleration is

$$\ddot{y}(t,u) = a(t,u) = a^0(t) + u\omega \cdot \Phi(t-t_0)\sin(\omega(t-t_0)) - u\omega \cdot \Phi(t-t_e)\sin(\omega(t-t_e))$$
$$a^0(t) = g\cos(\omega t) - v_0\omega\sin(\omega t) \qquad (6.4)$$

With this the restoring force of the rope is given by

$$F_R = m\omega^2(y-y_0) = -ma(t,u) + mg =$$
$$F_R^0 - um\omega \cdot \Phi(t-t_0)\sin(\omega(t-t_0)) + um\omega \cdot \Phi(t-t_e)\sin(\omega(t-t_e)) \qquad (6.5)$$

with $F_R^0 = mg - ma^0$. In the figure below, the reduction of the impact force by the rope control is illustrated for a typical fall.

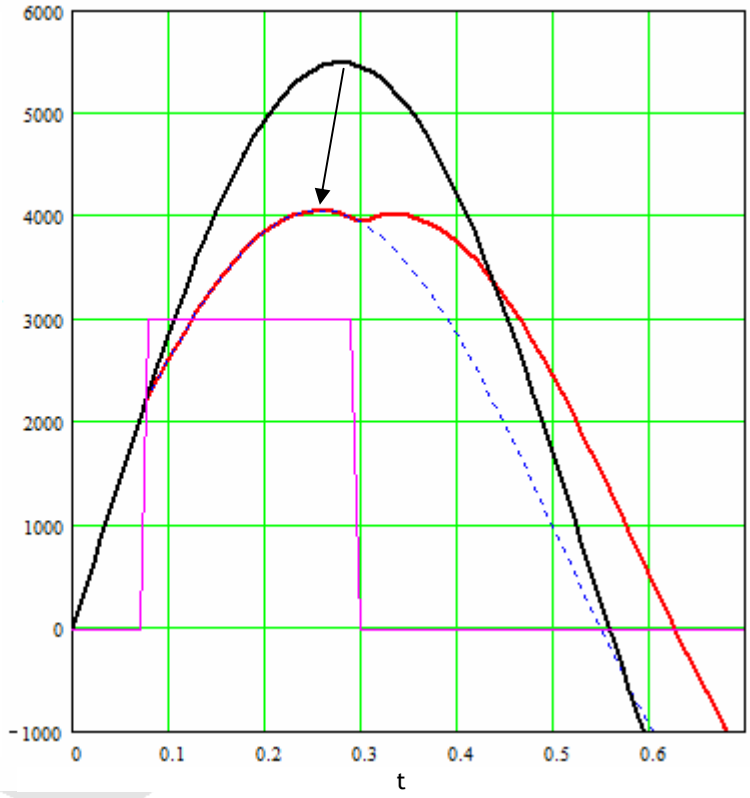

Fig.6-2: The black curve shows the time dependence of the impact force without control (u = 0). The red curve is the reduced impact force for t_0=0.075 sec and t_e=0.3 sec with u = 3m/sec. The difference between the red and the blue dashed curve is the additional force due to the stop of the rope. The speed of the rope slip u is 3000 mm/sec (magenta). (ω = 6.25 sec^{-1}, v_0 = 9.185 m/sec, s = 67.5 cm (equation (6.8)).

The impact force $F_R^0 = -ma^0(t) + mg$ for u = 0 stays positive far after the maximum of F_R and is therefore reduced by the negative second term in (6.5). The third term includes the "stopping

costs" and is exactly the time-shifted positive second term. One has, so to speak, to pay back the won reduction of the impact force at a later time which increases the time duration of the force. Nevertheless, the momentum (force integral over time) usually becomes smaller when u>0, because energy is withdrawn from the system by the rope slip. The law of energy conservation can be easily derived from (6.1) by multiplying this equation with $\dot{y}$ which leads to

$$\frac{d}{dt}\left[\frac{1}{2}m\dot{y}(t)^2 - mgy(t) + \frac{m\omega^2}{2}(y(t)-y_0(t))^2 + \int_0^t mu\omega^2(y(t')-y_0(t'))dt'\right] = 0 \qquad (6.6)$$

The last term $\int_0^t mu\omega^2(y(t')-y_0(t'))dt'$ is the energy which is absorbed by the belay device.

If the time of the maximum of a(t,u), t_a^{max}, is smaller than t_e, then we can write:

$$a(t,u) = g\cos(\omega t) - v_0\omega\sin(\omega t) + u\omega\sin(\omega(t-t_0)) =$$
$$(g - u\omega\sin(\omega t_0))\cos(\omega t) - (v_0 - u\cos(\omega t_0))\omega\sin(\omega t)$$

with the maximum impact force

$$F_1 = m\sqrt{(v_0 - u\cdot\cos(\omega t_0))^2\omega^2 + (g - u\omega\sin(\omega t_0))^2} + mg$$

and the limiting case of the complete rope slip when $u=v_0$ and $t_0=0$.

If the time $t_a^{max} > t_e$, then we have

$$F_2 = m\sqrt{(v_0 - u\cdot\cos(\omega t_0) + u\cdot\cos(\omega t_e))^2\omega^2 + (g - u\omega\sin(\omega t_0) + u\omega\sin(\omega t_e))^2} + mg$$

For the maximum of F_R there are only these 2 possibilities, so that

$$F_R^{max} = Max(F_1, F_2) \qquad (6.7)$$

The aim now is to make F_R^{max} as small as possible using the control parameters t_0 and t_e for a given rope slip

$$s = y_0^{max} = u\cdot(t_e - t_0) \qquad (6.8)$$

At the chosen t_0 and t_e and a given s, u is fixed and is thus no longer available as optimization parameter for the optimization of F_R^{max}.

The following Figure 6-3 shows the smallest possible F_R^{max} choosing the optimal t_0 and t_e. The control velocity u becomes constant for large s and is then about $2/3\cdot v_0$ (with the parameters of section 7). t_e is practically constant for small s<1 m and increases only for s >1 m. The effect of s on F_R^{max} is particularly large for 0 < s < 1 m and approaches zero for larger s.

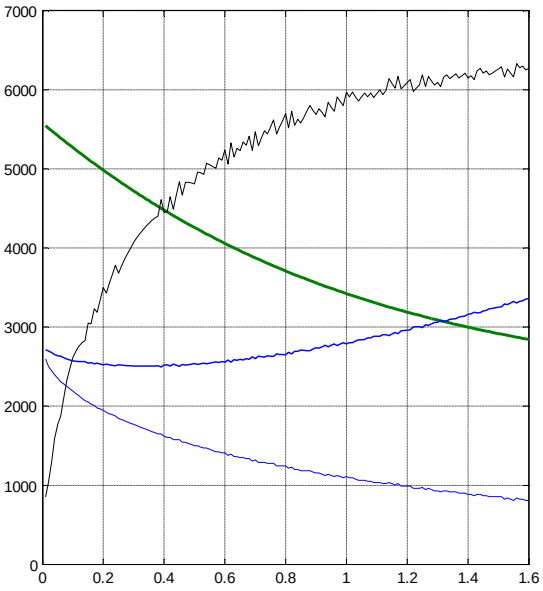

Fig.6-3: Optimal (smallest possible) maximum impact force F_R [N] (green) as a function of the rope slip s [m] and the associated t_0 [10^{-4} sec] (blue), t_e [10^{-4} sec] (blue), u [10^{-3} m/sec] (black).

Fig.6-4 shows the impact force with optimal control as a function of time. For comparison, the impact force without control (u=0) is plotted in blue.

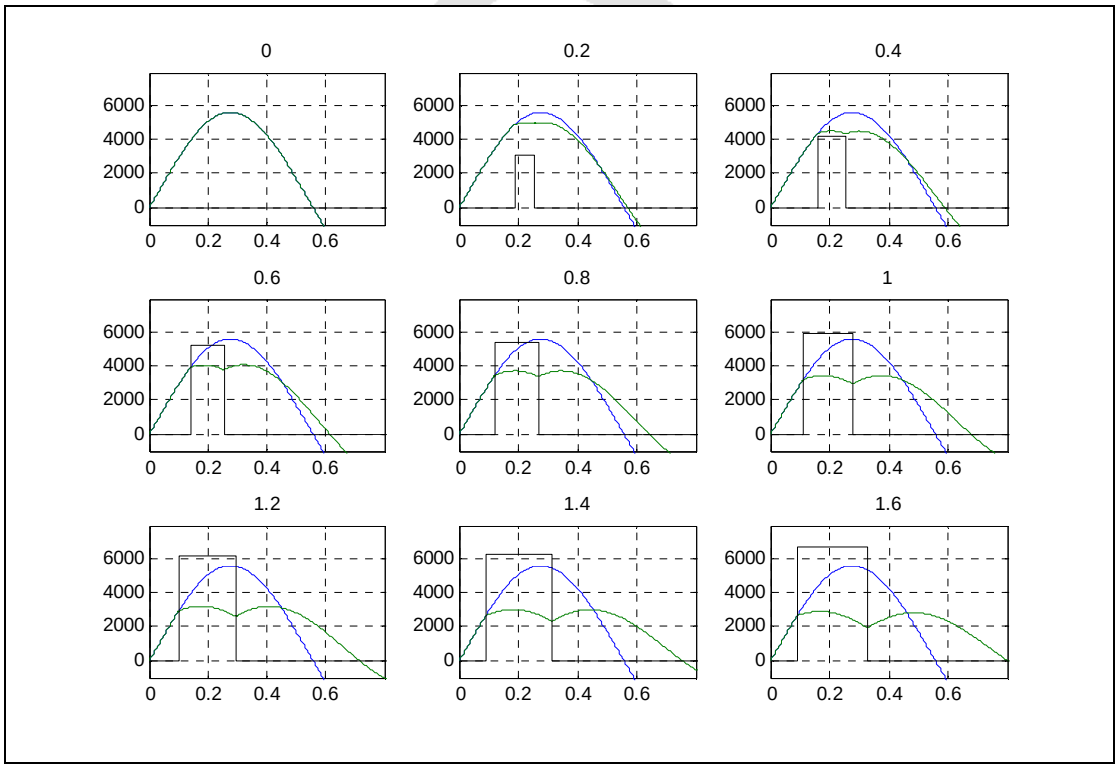

Fig.6-4: Time dependence of F_R (green) from equation (6.5) for 9 different distances of rope slip from 0 to 1.6 m. The parameters t_0 and t_e are chosen optimally. F_R^0 for u = 0 is plotted in blue as a reference curve. The black curves are the optimal rope slip velocities u [in 10^{-3} m / sec].

We also give an analytical approximation for the impact force reduction due to rope control. First, as can be seen from Fig.6-4, t_e is located always approximately at the maximum of F_R for u = 0, i.e. at about

$$t_e \cong \frac{\pi}{2\omega}.$$

Second, the two maxima of the impact force resp. the acceleration are always equal. As is intuitively clear, F_R^{max} is optimal when the two maxima of F_R become equal in size (see Fig.6-4). This provides a relation between t_0 and u:

$$t_0(u) = \frac{1}{\omega}\arcsin\left(\frac{1}{2}\left(1+\frac{2g}{u\omega}\right)\right). \tag{6.9}$$

Since F_R^{max} is given as a function of u, the following parametric equation between F_R^{max} and s is possible, with u as parameter:

$$\begin{pmatrix} s(u) = u\cdot\left(\frac{\pi}{2\omega} - t_0(u)\right) \\ F_R^{max}(u) \cong mg + m\sqrt{\left(u\sqrt{1-\left(\frac{1}{2}\left(1+\frac{2g}{\omega u}\right)^2\right)} - v_0\right)^2\omega^2 + \left(\frac{1}{2}u\omega\right)^2} \end{pmatrix} \tag{6.10}$$

This approximation is excellent for s ≤ 1 m.

For slightly smaller s, one can develop (6.10) for small s and one obtains for the impact force controlled by s:

$$F_R^{max}(s) \cong \left(mg + m\sqrt{v_0^2\omega^2 + g^2}\right)\cdot\left(1-\left(0.87\cdot\frac{\omega}{v_0} - 1.12\cdot\frac{g}{v_0^2}\right)s\right) \tag{6.11}$$

In this approximation, F_R^{max} is given by the familiar impact force formula $\left(mg + m\sqrt{v_0^2\omega^2 + g^2}\right)$, multiplied by a term linear in s whose strength is determined essentially by the factor ω/v_0. It is also intuitively clear that a particular s has a greater effect on a stiff rope with a large ω than on a rope with a smaller ω. A large v_0, on the other hand, requires a larger s for the same impact force reduction.

Looking at (6.11) for a slack rope of length δ (which some climbers regard as a kind of control), one must change $v_0 = \sqrt{2gh}$ to $v_0 = \sqrt{2g(h+\delta)}$ because the fall height h is increased by the slack δ. On the other hand, $\omega = \sqrt{k/m}$ contains the length dependent k = $EL_0/(L+\delta)$ which is slightly reduced by δ, so that for small δ/L one gets

$$F_R^{max}(0) = mg + m\sqrt{v_0^2\omega^2 + g^2} \approx mg + \sqrt{2mgEq\cdot\left(f + (1-f)\frac{\delta}{L}\right) + (mg)^2} \tag{6.12}$$

which for a fall factor f > 1, surprisingly, is reduced by slack rope. For single pitch routes, however, a fall factor f > 1 is not possible, so that slack rope must always be avoided in places where it is most commonly observed, namely in the climbing gym or the climbing garden.

We also discuss a simple model for the case when the belay device is attached to the harness as shown in figure 6-5. During a fall the belayer with mass m_0 is pulled up by the mass m of the falling climber. The belayer can jump upward with a velocity u and can thus control the fall. In the approximation of the undamped harmonic oscillator model ($\omega = \sqrt{k/m}$) one gets the following nice formula for the impact force which is presented without derivation:

$$\tilde{F}_R^{HO} = m_{red}\,2g + m_{red}\cdot\sqrt{\Omega^2\cdot(v_0-u)^2+(2g)^2} \quad \text{with} \quad m_{red} = \frac{m\cdot m_0}{m_0+m} \quad \text{und} \quad \Omega^2 = \frac{k}{m_{red}}\ ,$$

This is to be compared with the familiar impact force formula (6.12) (see [1]):

$$F_R^{HO} = mg + m\sqrt{v_0^2\omega^2+g^2}\ .$$

m_{red} is the reduced mass and, since it is always less than m, it reduces the impact force. Ω will be always larger than ω because of m_{red}, so that the falls become shorter in time. u reduces the initial velocity v_0 of the falling climber, thus reduces also the impact force.

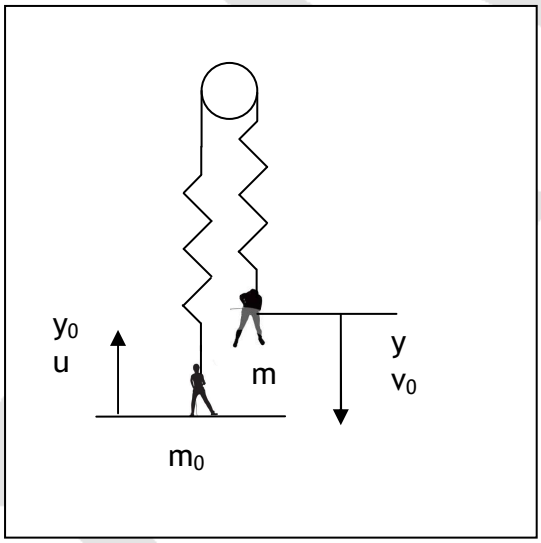

Fig.6-5: Simple model for belaying off the harness

6.2. Rope control with internal and external friction

Similar to Fig.6-4, F_R is shown in Fig.6-6 as a function of time using optimal rope control, when both types of friction are present. The graphs are the result of the solution of the equation system (4.4), followed by the minimization of F_R^{max} as a function of rope slip y_0. The parameters used are those of section 6.1.

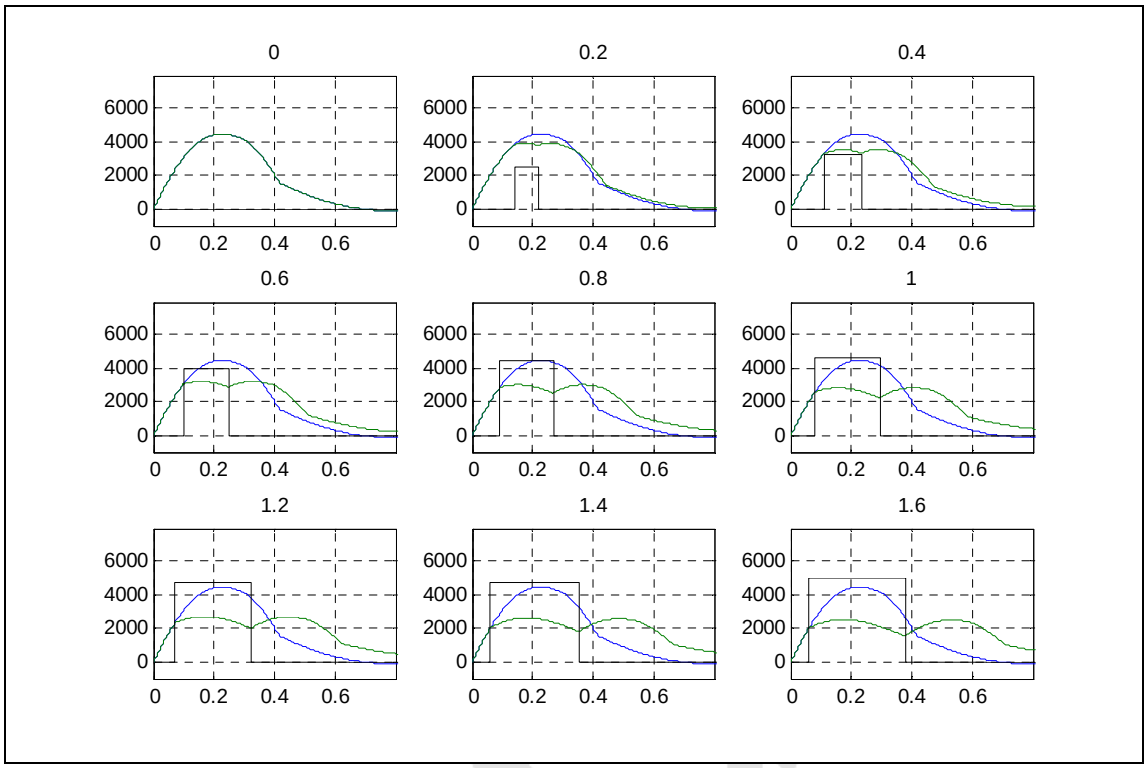

Fig.6-6: Time dependence of F_R (green) from equations (4.4) for 9 different slide distances of the rope from 0 to 1.6 m. The internal friction is $\eta=0.8\cdot10^3$ [Nsec/m], the external friction is $\rho=1.46$. The parameters t_0 and t_e are chosen optimally, so that the maximum of F_R is minimized. F_R^0 for u = 0 is plotted as reference curve in blue. The black curves are the optimal rope slip velocities u [10^{-3} m/sec].

Note that for larger s > 1 m no significant reduction of the impact force occurs (see the three lowest figures in 6-6). Moreover, the relatively early stop of the rope slip is remarkable (see Fig.6-7): when the slide times are too long, the force is no longer reduced but only prolonged. In addition, long slide distances feed energy to the system "climber + rope" that must also be converted into heat.

A typical "force controlled" belay device will not stop near the force maximum, but only when the force falls below a certain limit. Probably this is the reason why the experimental impact force reductions are not optimal (see Section 7, Figure 7-9).

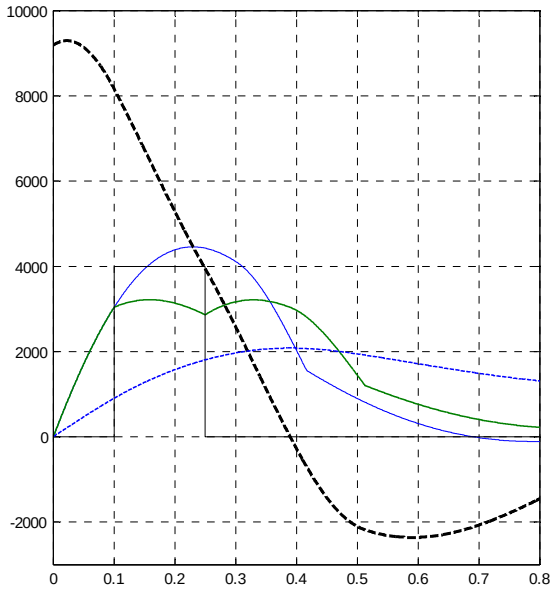

Fig.6-7: Enlarged fourth figure of Fig.6-6 with s = 60 cm. The end of the optimal rope slip y_0 occurs at an early stage near the force maximum, although the falling mass still has a high speed (dashed black) and the maximum elongation (dashed blue)is far from being reached.

In the next Figure 6-8, the time variation of all dissipative energies is shown. These are all of equal magnitude and add up to the total energy for times slightly larger than 1 sec.

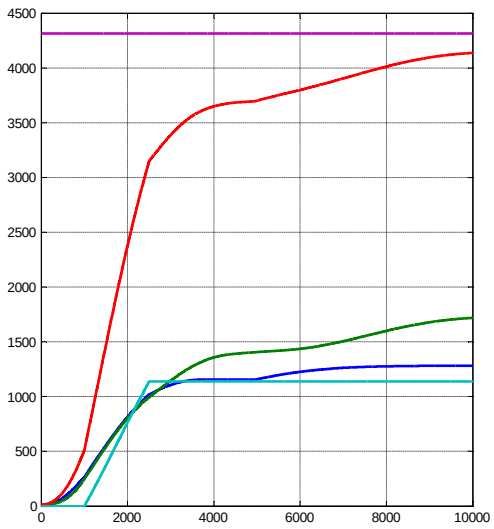

Fig.6-8: Time dependence in [10^{-4} sec] of the energy absorption at the belayer (cyan), by internal (green) and external friction (blue). The sum of all three dissipative energies is the red curve that asymptotically approaches the total energy (magenta). The rope slip is 51 cm.

7. Comparison with experiments

In this section we compare the theoretical results, especially the solution of the equation system (4.4), with measurements carried out by the DAV Sicherheitsforschung [3].

The fall experiments are characterized by:

Falling mass m = 82 [kg]
Initial velocity of the falling mass v_0 = 9.185 [m/sec]
Rope length in front of the anchor point L1 = 6.95 [m]
Rope length behind the anchor point L2 = 3.4 [m] (7.1)
Total rope length L = 10.35 [m]
Parameter for the external friction ρ = 1.46

All measurements discussed herein are based on a rope with the following parameters:

$k_2 = 3.2 \cdot 10^3$ [N/m], $k_1 = 1.8 \cdot 10^3$ [N/m], $\eta \frac{q}{L} = 0.8 \cdot 10^3$ [Nsec/m].

corresponding to

E2 = 0.42 [GPa], E1 = 0.24 [GPa], η = 0.1 [GPasec]

Figure 7-1 shows the measured curves of F_R and F_S and the associated curves from the theory as a function of time. The rope slip for this experiment is only a few centimeters and therefore negligible.

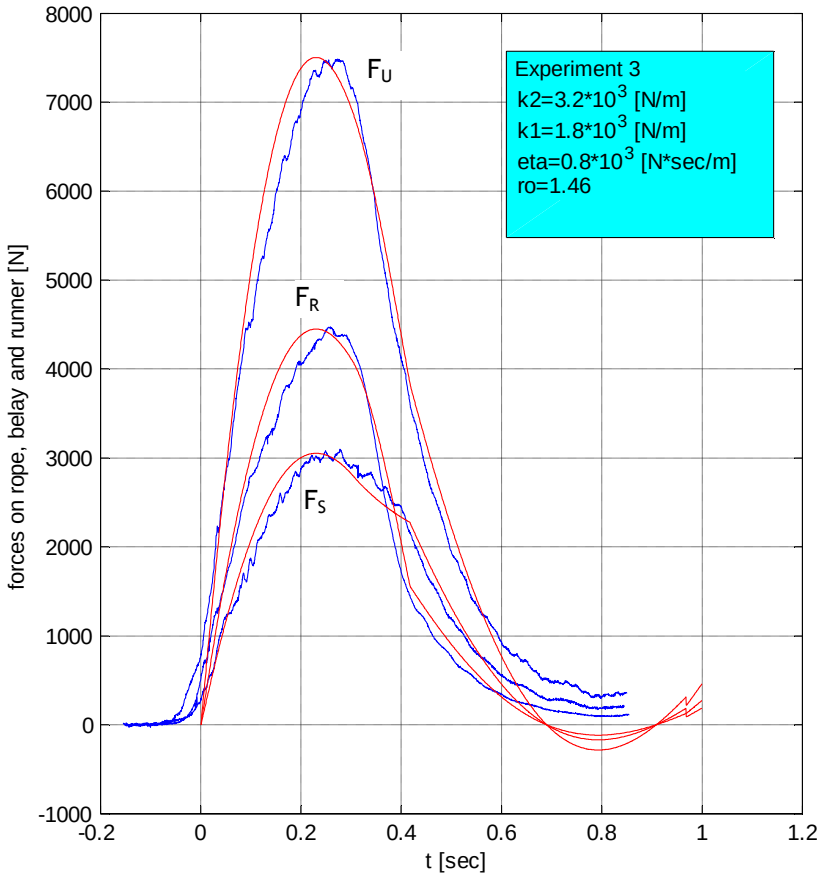

Fig.7-1: F_R, F_S and their sum F_U at the anchor point when rope slip is neligible s ≈ 0. Measurements in blue, theoretical curves in red.

For the above experiment, the (not measured) elongation y_{22} at the falling mass, its velocity v_{22} and its acceleration $-a_{22}$ are shown in Fig.7-2.

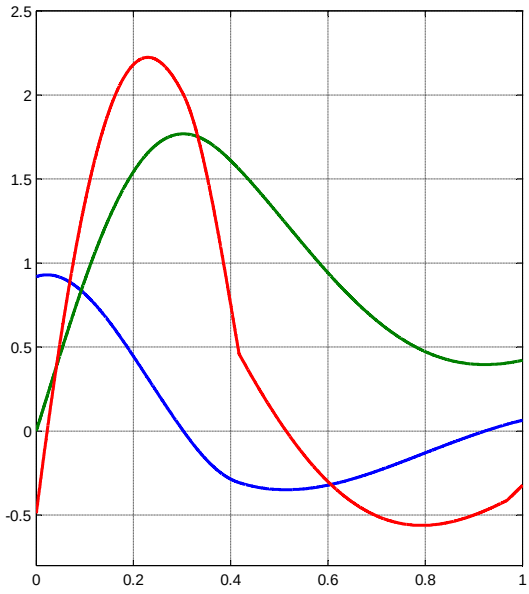

Fig.7-2: Rope elongation y_{22} [m] at the falling mass (green), its velocity v_{22} [10m/sec] (blue) and its acceleration $-a_{22}$ [20m/sec^2] (red) as a function of time.

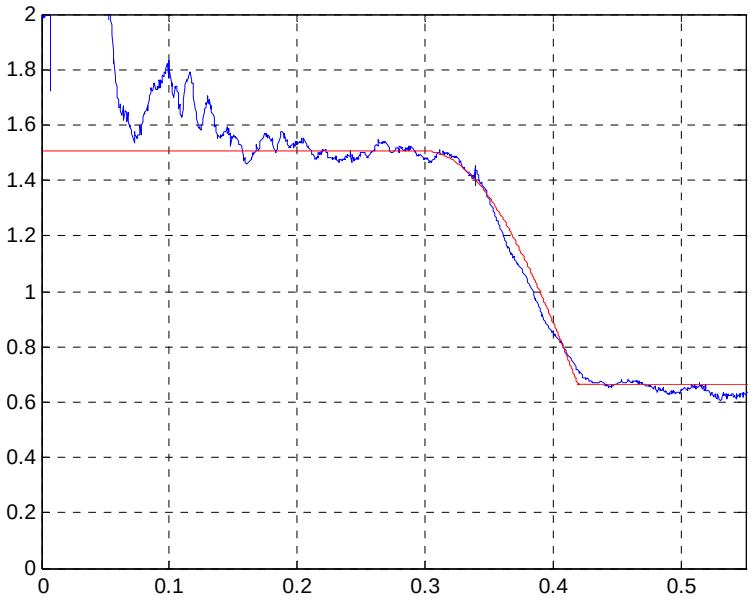

Figb.7-3: The ratio impact force – belay force

For the same experiment (s = 0), Fig.7-3 shows the measured (blue) and calculated (red) ratio F_R/F_S of impact force to force on the belay. It was shown in section 2 that $\rho = F_R/F_S$ is valid before the change of sign of the velocity and $F_R/F_S = 1/\rho$ afterwards which is confirmed experimentally. In Figure 7-4, the friction force $R = F_S - F_R$ is shown. Again, the good

agreement with the experiment indicates that the used simple Coulomb model of friction describes correctly a real fall.

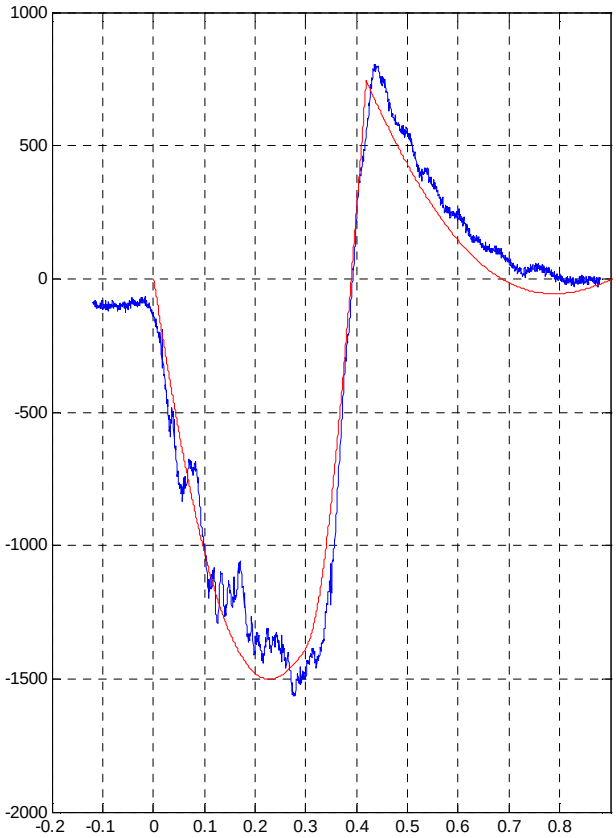

Fig.7-4: Friction force R as a function of time

We now show 4 fall experiments with a larger rope slip s (increasing from 44 cm to 91 cm) and compare them with the theoretical results.

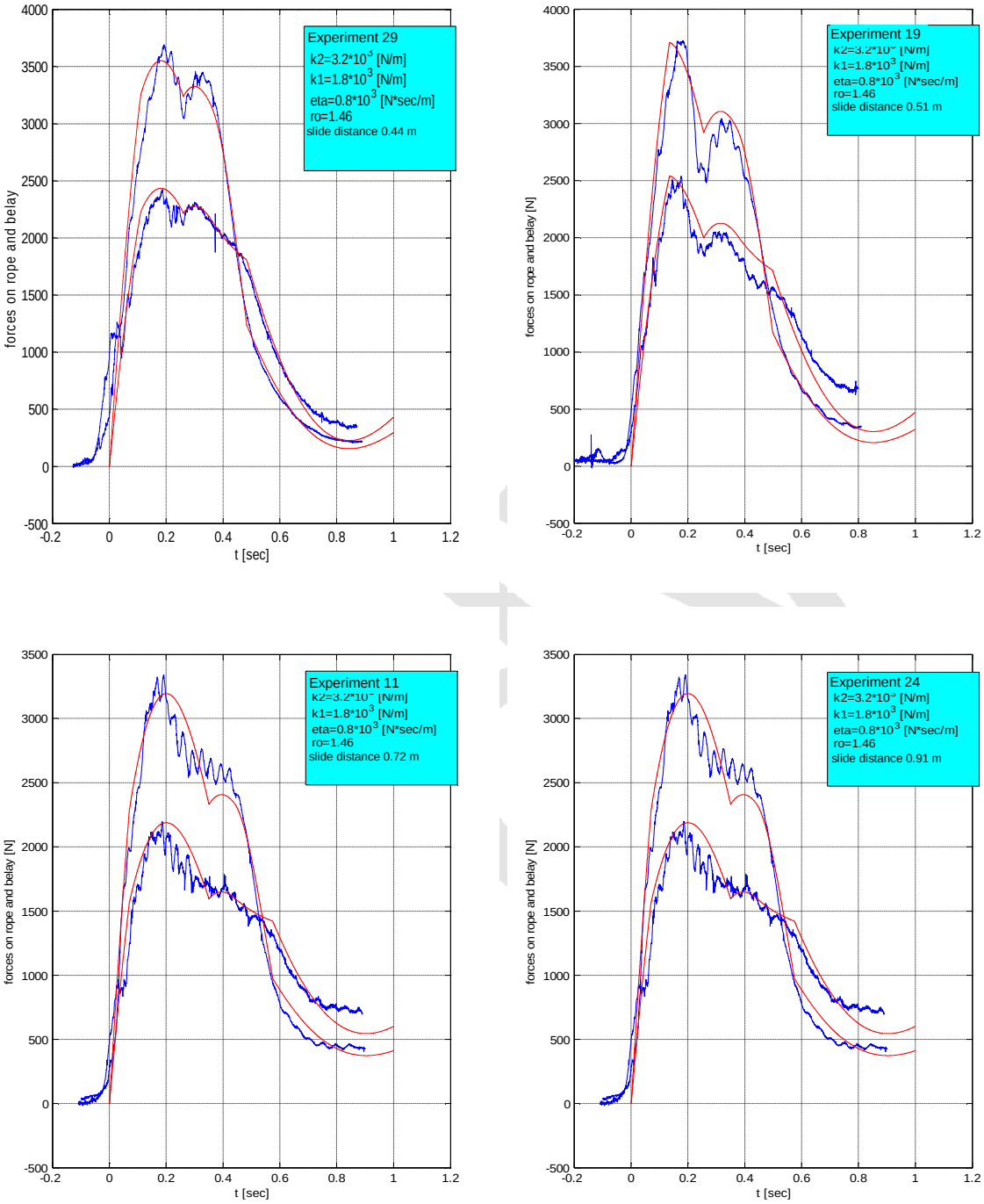

Figs.7-5 to 7-8: Measured curves (blue) and theoretical curves (red) for F_R and F_S as a function of time for various slide distances s.

In the next Fig.7-9, all available experimental reductions of the relative impact force $F_R^{max}(s)/F_R^{max}(0)$ are shown as circles. $F_R^{max}(0)$ was obtained by averaging over 4 identical experiments, so that $F_R^{max}(s)/F_R^{max}(0)$ can even become slightly larger than one for $s \to 0$. The red curve is the maximum possible theoretical reduction of the impact force at a given s. The measured values must always be above or on this curve which is fulfilled except for one point.

It is striking that the measured reductions of impact force have a large spread and are clearly away from the optimal curve.

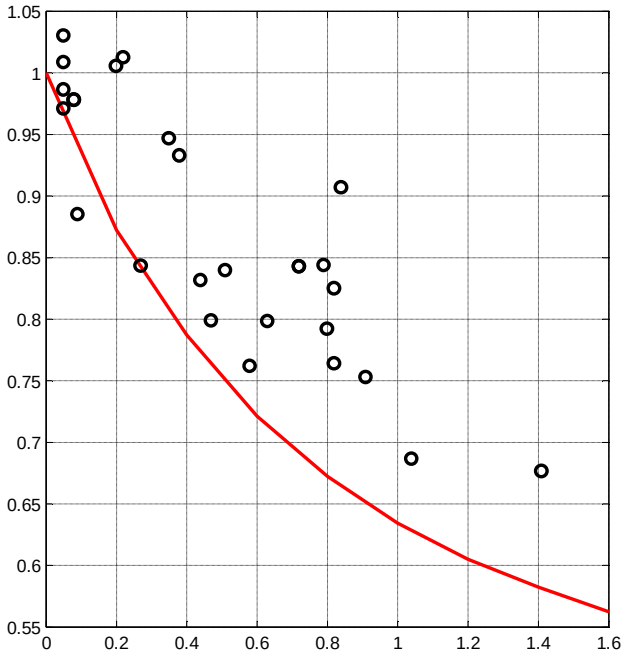

Fig.7-9: Reduction of impact force as a function of the rope slip for a total of 27 experiments (circles) and the theoretically maximum possible reduction (red curve). Most of the real world, controlled impact forces are clearly away from optimality.

8. Conclusions

The good agreement between theory and experiment shows that a linear viscoelastic SLS-model provides a very good description of a climbing rope. We could explain a whole series of different fall experiments with a specific rope that is characterized by two parameters (one modulus of elasticity and the viscosity; the second modulus of elasticity is only of minor importance for short times).

The added external friction, which is also correctly described by our model and which can explain the measurements, turns the previously linear model into a nonlinear, more complex model. The figures 8-1 below show that both types of friction, external and internal, are important for typical falls with not too high fall factors.

The familiar model of the harmonic oscillator (Fig. 8-1a) is insufficient to explain the forces that occur during a fall. The external friction (Fig. 8-1b) is responsible for the difference between the forces F_R and F_S. An increasing external friction leads to an increase of the force F_R and to a decrease of the force F_S on the belay with lower control possibilities of the belayer.

The internal friction (Fig.8-1c) is important for the absorption of the fall energy, thus preventing the oscillation of the rope and also reducing F_R substantially. Both types of friction combined (see Fig. 8-1d) can explain the forces on the falling mass and on the belayer well.

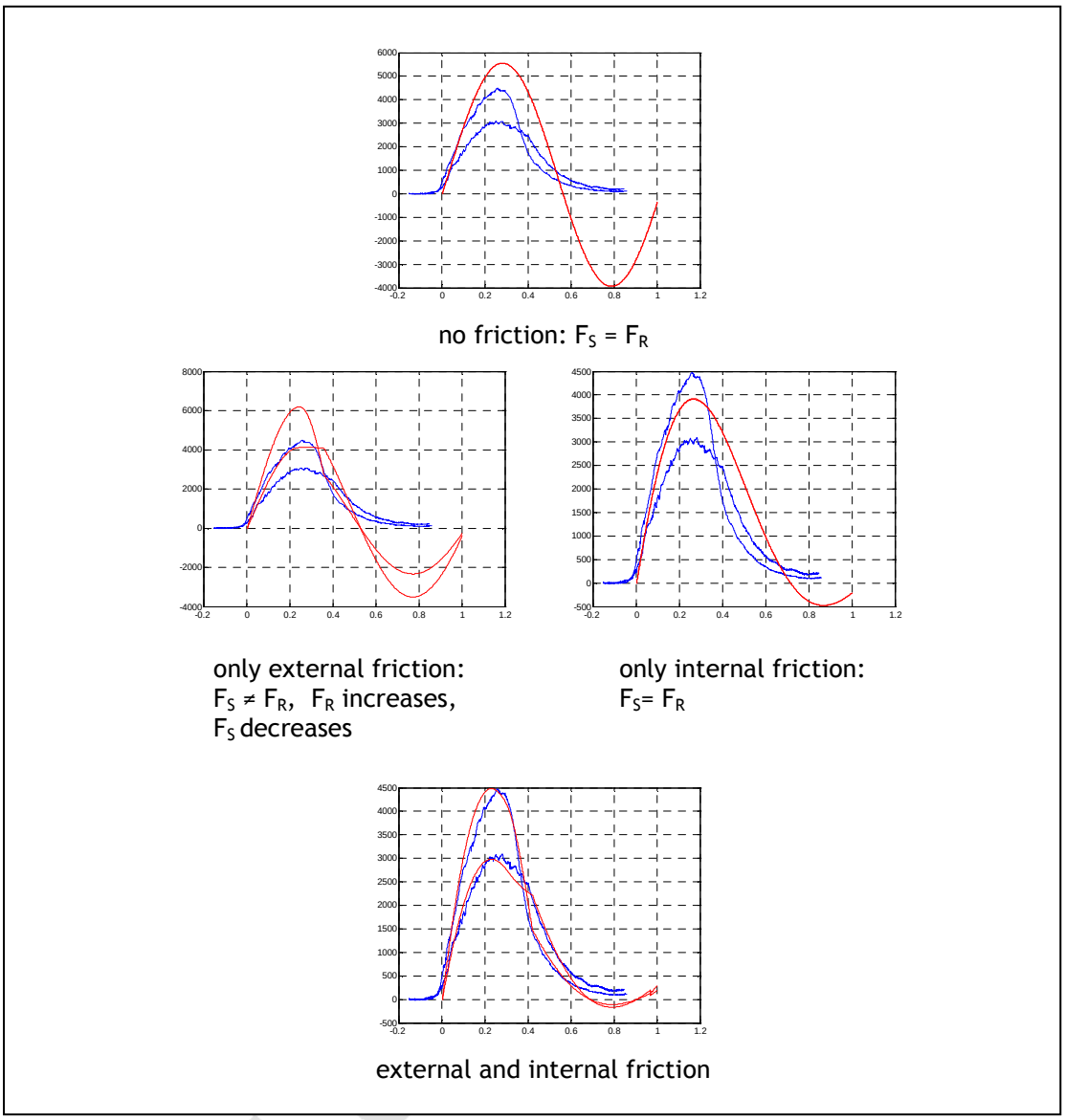

Fig.8-1a,b,c,d: Forces on the falling mass and on the belay as a function of time. The theoretically calculated curves are in red, the experimental, always identical reference curves, are in blue.

An important part of the paper examines the reduction of the maximum impact force through the control of the belayer. The optimal rope control (with the best possible reduction at a given rope slip) allows a significant reduction of the impact force even at moderate slide distances (see Fig.7-9) and is carried out by stopping the rope slip relatively early near the maximum of the impact force. Since belay devices apparently fail to follow the optimal start and stop times, they can provide virtually only suboptimal results.

9. Acknowledgment

I particularly thank Chris Semmel of the DAV Sicherheitsforschung who kindly provided me with the measurement results.

